A Torque Ripple Minimization Method for Six-Phase Switched Reluctance Motor Drives

Xu Deng, Barrie Mecrow, Shady Gadoue and Richard Martin

Abstract -- **This paper presents a direct torque control (DTC) method on a six-phase SRM driven by a six-phase asymmetric half bridge converter. Modeling and simulations of the proposed drive system have been built with MATLAB/SIMULINK. In the proposed DTC method, instantaneous output torque of the six-phase SRM is directly controlled by flux-linkage magnitude and rotating speed regulation (acceleration or deceleration) respective to rotor movement. The simulation and test results accurately reflect the actual operation states of the SRM. Compared with traditional current chopping control (CCC), the DTC method can effectively reduce the torque ripple for the six-phase SRM.**

Index Terms— **Current chopping control, Direct torque control, Switched reluctance motor, Torque ripple**

I. INTRODUCTION

S RMs have the simplest structure of all electrical motors [1] and have been developed for many applications, such as aerospace generators, high-speed drives, small automotive applications, cooling fans and pumps [2-4]. In recent years, the high price of rare-earth materials has renewed interest in SRMs for hybrid electric vehicles, which have previously employed permanent magnet synchronous machines [5, 6]. In addition, the SRM has a high fault-tolerance due to the ability to operate with the loss of one or more motor phases [7, 8].

However, SRMs have highly nonlinear magnetization characteristics due to the doubly salient structure, and torque ripple is a major drawback [9]. Traditional control methods such as current chopping control (CCC) and angle position control aim at producing a command average torque without minimizing torque ripple, thus large torque ripple is produced during dynamic operation. In order to solve this problem, many investigations have been undertaken on machine optimization [10-12] and advanced control strategies [13-16].

The structural parameters of SRMs, such as the air gap, length and shape of the rotor and stator poles, stator winding turns, iron core length and pole arcs have a significant impact on torque ripple. By designing a new stator pole face with a nonlinear air-gap and a pole shoe attached to the lateral face of the rotor pole, undesired torque ripple is reduced in [10]. By inserting one punching hole in each rotor pole to modify the waveforms of flux as well as derivatives of sinusoidal inductances, higher average torque and lower torque ripple

was reported in [11]. A nonlinear air gap with asymmetric inductance profile is considered in [12], with this design a flat topped torque with a low torque ripple is obtained.

As the phase number rises, the number of torque pulses per cycle increases, thereby reducing the torque ripple. Multi-phase machines have appeared in last two decades [17] as a simple way to reduce torque ripple. However, in most cases there are more power devices, increasing the cost and complexity of the drive. Recently a six-phase 12/10 pole SRM was reported [18]. A standard three-phase full bridge converter is employed to drive this SRM with sinusoidal voltages. Compared with traditional three-phase SRMs, torque ripple is reduced [19, 20].

To further reduce torque ripple, lots of advanced control strategies have been investigated. The majority of them focus on modulation of the phase currents or voltage profiles to generate a specific torque command. In these methods, to reduce the torque ripple it is necessary to regulate the torque production of every individual phase. The torque reference is distributed into each phase torque reference according to the rotor position by a torque sharing function [13]. In addition, iterative learning and neural network methods have been employed [15, 16]. However, these control schemes require complex computation and are hard to implement in real-time systems.

Direct torque control (DTC) techniques have been applied to induction machines and permanent magnet machines [21, 22]. In order to simplify the control method, the principle of DTC of AC machines was then applied to SRM drives [23]. In this method, the magnitude of the flux-linkage is kept within a hysteresis band, while torque is directly controlled by accelerating or decelerating the flux-linkage vector with respect to the rotor position.

In this paper a DTC method for a six-phase 12/10 pole SRM is researched. The stator flux arrangement and its estimation method is proposed, meanwhile voltage vectors for the ix-phase SRM and their selection principle are also discussed. A dynamic drive system has been built in the MATLAB/SIMULINK environment with measured nonlinear electromagnetic flux and torque characteristics of this six-phase SRM. Simulation results show that instantaneous torque and stator flux-linkages have more linear waveforms than with current controllers. Whilst producing the same average torque output, the proposed DTC method can significantly reduce torque ripple for the six-phase SRM in experimental test.

Xu Deng, Barrie Mecrow, Shady Gadoue and Richard Martin are with the School of Electrical and Electronic Engineering, Newcastle University, UK (e-mail:x.deng4@ncl.ac.uk).

II. THE BASIC PRINCIPLE OF DTC FOR SRMs

The instantaneous torque of SRMs can be described as (1), in which W_m, W_e and W_f are mechanical energy, electrical energy and field energy respectively [23].

$$T = \frac{dW_m}{d\theta}\bigg|_{i=const} = \frac{d(W_e - W_f)}{d\theta}\bigg|_{i=const}$$
$$= \frac{dW_e}{d\theta}\bigg|_{i=const} - \frac{dW_f}{d\theta}\bigg|_{i=const} \qquad (1)$$
$$= i\frac{\partial\varphi(\theta,i)}{\partial\theta} - \frac{\partial W_f}{\partial\theta}\bigg|_{i=const}$$

For a given current the flux-linkage and the magnetic stored energy both rise as the rotor comes into alignment and both fall once past alignment, i.e. they both always have the same polarity. Furthermore, the magnitude of the rate of change of stored energy will always be less than the $i\frac{\partial\varphi(\theta,i)}{\partial\theta}$ term. Consequently, as the direction of the current is always positive, the polarity of the torque is always the same as the polarity of $\frac{\partial\varphi(\theta,i)}{\partial\theta}$. If $\frac{\partial\varphi(\theta,i)}{\partial\theta} < 0$, the instantaneous torque $T < 0$, and vice versa. In other words, to produce a positive torque the stator flux amplitude should increase with respect to rotor position, whereas to produce a negative torque the stator flux amplitude should decrease with respect to the rotor position. A positive value of $\frac{\partial\varphi(\theta,i)}{\partial\theta}$ is defined as flux acceleration, whereas a negative value of $\frac{\partial\varphi(\theta,i)}{\partial\theta}$ is defined as flux deceleration. Hence, the DTC control technique for SRMs is as follows:

(a) The stator flux-linkage vector of the motor is kept at a constant by selecting an appropriate voltage vector.

(b) The torque can be controlled by accelerating or decelerating the stator flux vector relative to the rotor movement.

III. THE DTC METHOD FOR SIX-PHASE SRMs

A six-phase asymmetric half-bridge power converter for a six-phase SRM is shown in Fig. 1. According to the on-off states of the IGBTs, each phase winding has three voltage states. When S1 and S2 are on the winding voltage is positive and this state is defined as +1. When S1 (or S2) is off the winding is short-circuited through S2 (or S1) and D2 (or D1), the winding voltage is zero and this state is defined as 0. When S1 and S2 are off the winding freewheels through D1 and D2, the winding voltage is negative and this state is defined as −1.
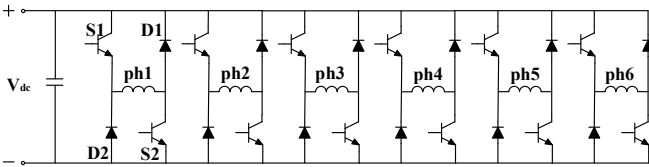

Fig. 1. A six-phase asymmetric half-bridge power converter

At any moment, each phase winding is in a specific voltage state and a voltage vector can be created by the common action of six-phases. The direction of the voltage time vector of phase k is consistently selected with the flux space vector of phase k in the time-space coordinate system to form the voltage vector U. The six-phase SRM has six stator flux directions, equally spaced by 60 electrical degrees. At any one instant these fluxes can be increased by applying a positive voltage or decreased by a negative voltage. In Fig. 2 the flux is split into 12 sectors. There are effectively 12 voltage vectors, U1 to U12, as shown in Fig. 2, representing the positive and negative voltages which can be applied to each phase. In addition, the time-space coordinate system is divided into 12 zones, N1 to N12. Each zone spans 30 electrical degrees and each voltage vector is located on the central axis of a zone.
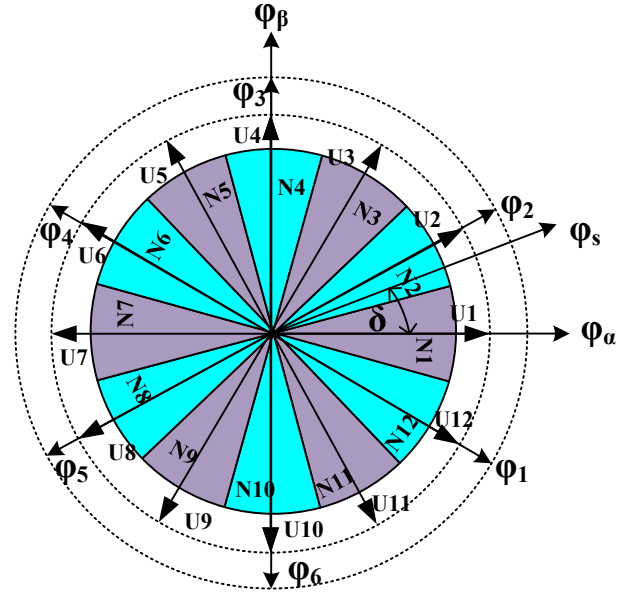
U1 (+1,+1, 0 ,-1,-1, 0)	U7 (-1,-1, 0 ,+1,+1, 0)
U2 (+1,+1,+1,-1,-1,-1)	U8 (-1,-1,-1,+1,+1,+1)
U3 (0,+1,+1, 0 ,-1,-1)	U9 (0,-1,-1, 0 ,+1,+1)
U4 (-1,+1,+1,+1,-1,-1)	U10 (+1,-1,-1,-1,+1,+1)
U5 (-1, 0 ,+1,+1, 0 ,-1)	U11 (+1, 0 ,-1,-1, 0 ,+1)
U6 (-1,-1,+1,+1,+1,-1)	U12 (+1,+1,-1,-1,-1,+1)

Fig. 2. Flux arrangement and relationships with voltage vectors

According to the DTC principle, the amplitude and position of the stator flux-linkage must be controlled by selecting an appropriate voltage vector. For this purpose the flux-linkage discrete expressions need to be produced. Equation (2) is written in difference form. Increasing or decreasing of stator flux depends on the angle between previous stator flux $\Psi(k-1)$ and new voltage vector $U(k)$, while the change of torque depends on the position of $U(k)$ respect to $\Psi(k-1)$.

$$\Psi(k) = \Psi(k-1) + U(k) \cdot T_s \qquad (2)$$

To further explain how to choose a suitable voltage vector, this section assumes stator flux is in zone N2 as an example. If both stator flux and instantaneous torque need to increase, U1, U3, U4 and U12 can be chosen to increase flux, while U2 to U6 can be chosen to increase torque. Hence only

U3 and U4 can increase flux and torque at the same time, and in order to achieve a rapid response and less switching loss, U3 is chosen in this case. The switching rule to realize DTC for a six-phase SRM is shown in Table I. In general, to increase both flux and torque, the voltage should be applied in the next sector, (k+1), whilst to reduce flux and torque it should be applied five sectors behind, (k-5). If stator flux and instantaneous torque have different changing command, the voltage vector chose to increase the torque should be near the current sector as long as it can fulfill the flux changing command as well, and vice versa. Thus, to increase torque and decrease flux, the voltage should be applied 4 sectors ahead, (k+4), whilst to reduce torque and increase flux it should be applied two sectors behind, (k-2).

TABLE I
SWITCHING TABLE FOR SIX-PHASE SRMs

$\Psi\uparrow T\uparrow$	$\Psi\uparrow T\downarrow$	$\Psi\downarrow T\uparrow$	$\Psi\downarrow T\downarrow$
$U(k+1)$	$U(k-2)$	$U(k+4)$	$U(k-5)$

The control diagram used for the DTC method is shown in Fig. 3. Six phase currents and voltages are measured by sensors and rotor position is fed back from the encoder. The six individual phase fluxes can be achieved from integration using the measured phase currents and phase voltages according to (2). Then the six phase fluxes are simply resolved onto the α-β frame according to their position relationships. From this both the magnitude and angle of the stator flux are achieved. Instantaneous torque can be calculated from the current and rotor position, using measured static nonlinear torque characteristics. By comparing the flux and torque references with estimated values, the optimum voltage vector is chosen according to the switching table, Table 1, and is applied to the inverter.
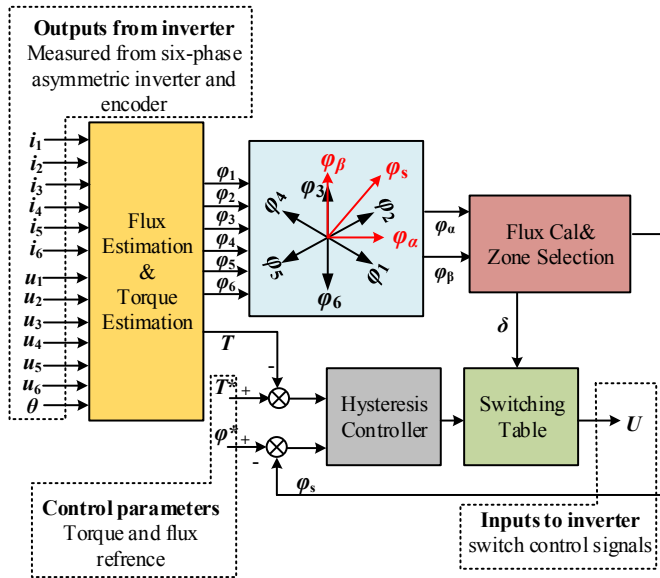

Fig. 3. Control diagram of DTC method for a six-phase SRM

IV. SIMULATION RESULTS

In order to compare the proposed control method with a traditional control method, a dynamic model of a six-phase SRM is developed in MATLAB/SIMULINK environment. This model uses parameters of a 12/10 six-phase SRM prototype. Fig. 4 shows the electromagnetic properties of this SRM prototype. Different control strategies are carried out and the following results are obtained to analyze the performance of the CCC and DTC methods.
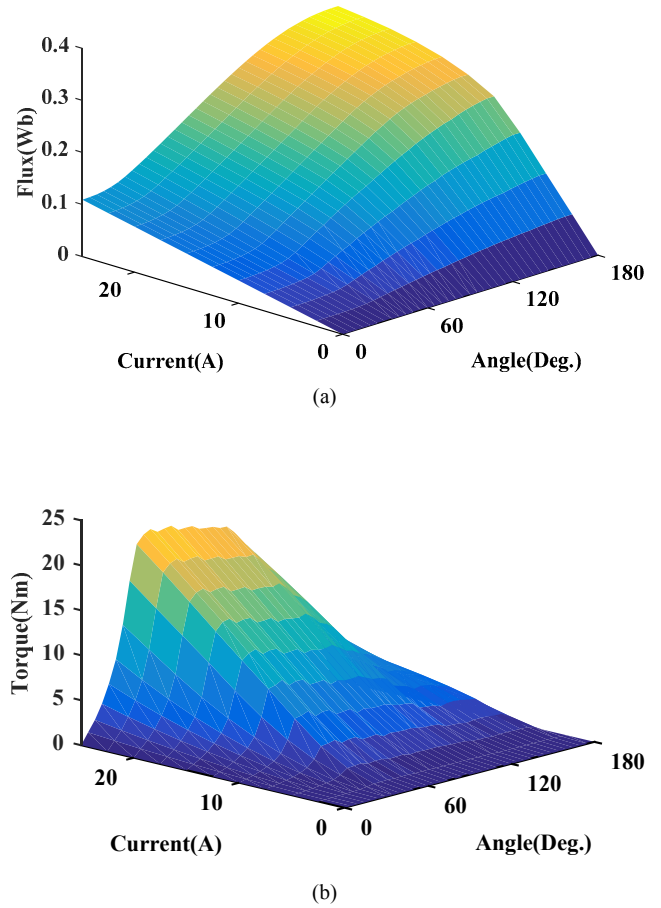

(a)

(b)

Fig. 4. Measured nonlinear electromagnetic characteristics of a six-phase SRM: (a) relationship between rotor position, current and flux, (b) relationship between rotor position, current and torque

Simulation parameter settings are as follows: DC power supply voltage is 560V, rotational speed is 1500 rpm. In the DTC method the flux reference is 0.34Wb, the torque reference is 15Nm, and the hysteresis bands for flux and torque are 0.02Wb and 0.5Nm respectively. In CCC method, the on and off angle is 0º and 165º respectively, the current reference is 12.5A and the hysteresis band for current is 0.5A. In the simulations, both CCC and DTC method have a fixed 10 kHz control frequency.

Fig. 5 shows simulation results of the CCC method, including phase flux, phase current, and phase torque. With the CCC method, only phase current is controlled by hysteresis controllers, thus phase flux and phase torque are nonlinear waveforms.

Fig. 6 shows simulation results of the DTC method, including phase flux, phase current, and phase torque. With the DTC method, both stator flux and instantaneous torque are controlled by hysteresis controllers, therefore phase flux and torque become more linear. However, with the same RMS current which is 8.3A, the maximum phase current of DTC method increases to 18A, whilst only 13A is needed with the CCC method. Therefore, a higher current ripple appears in the DC link, which has consequences for the DC power supply.
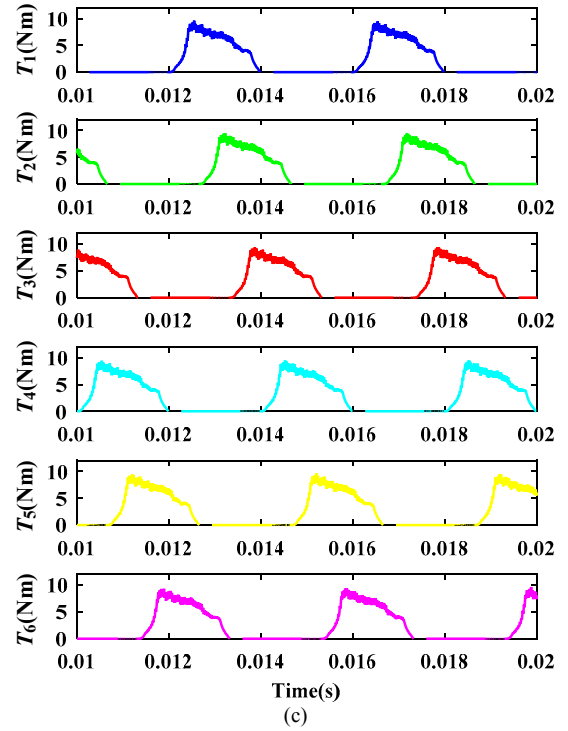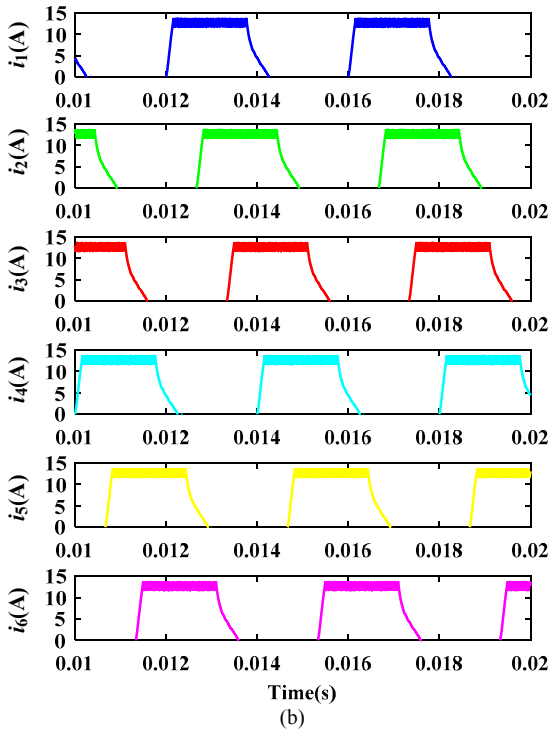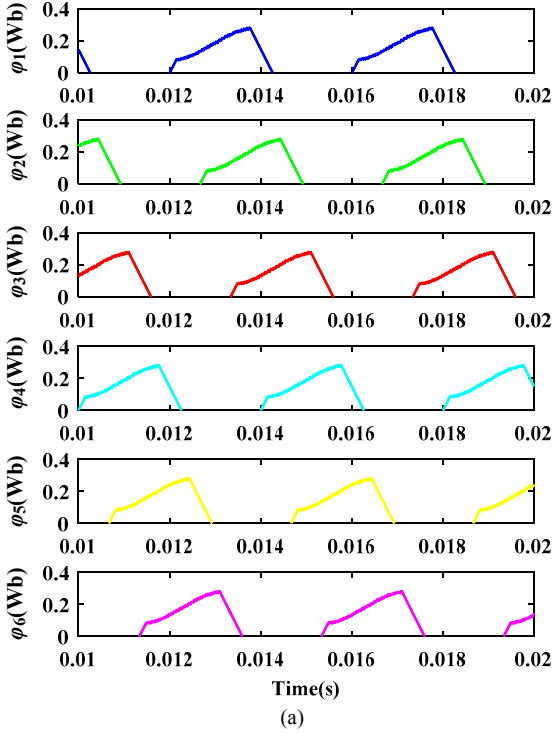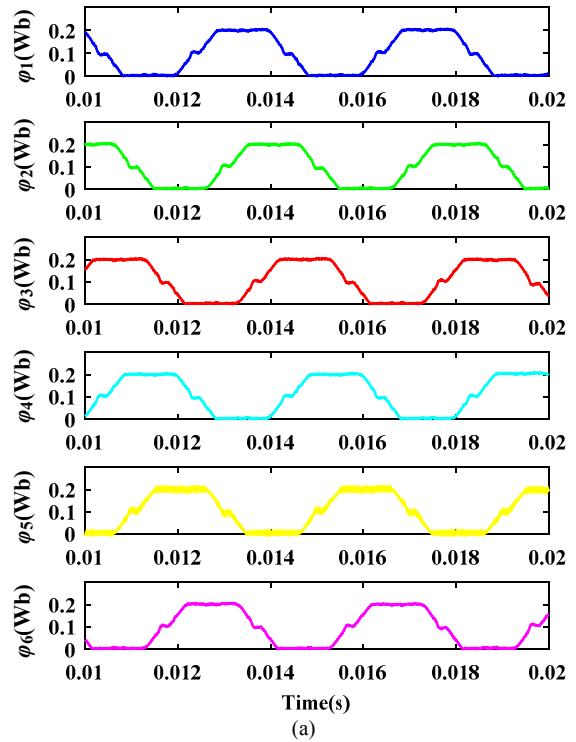

(a)

(b)

(c)

Fig. 5.   Simulation results of CCC method: (a) six phase flux, (b) six phase current, (c) six phase torque
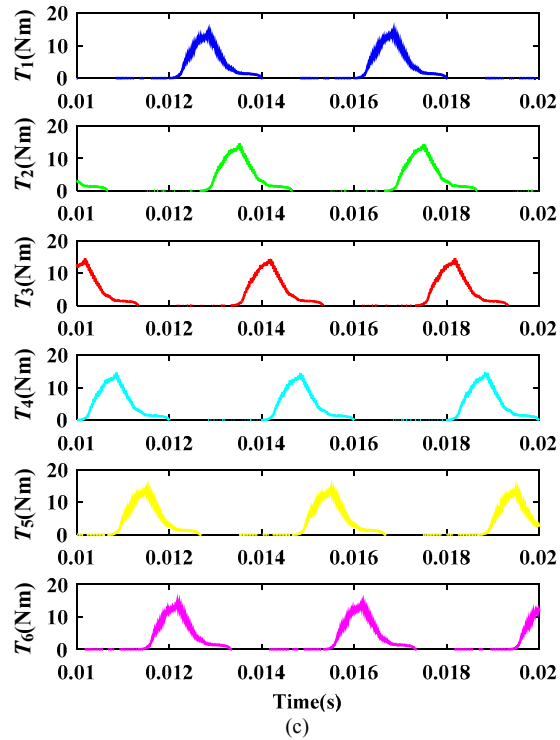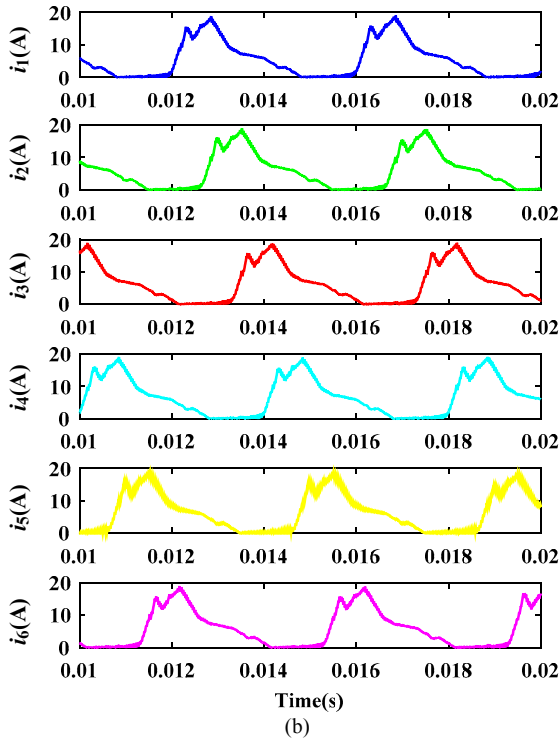

(a)

Fig. 6. Simulation results of DTC method: (a) six phase flux, (b) six phase current, (c) six phase torque

Fig. 7 shows the stator flux amplitude and total torque output with the CCC and DTC method. The stator flux-linkage with DTC is controlled within a 0.02Wb band according to the flux reference value, while with the CCC method it is a repeated nonlinear waveform and has a higher average value. Producing the same average torque of 15.1Nm, torque ripple in the CCC method is 50.6%, whilst the DTC method reduces it to 18.6%.
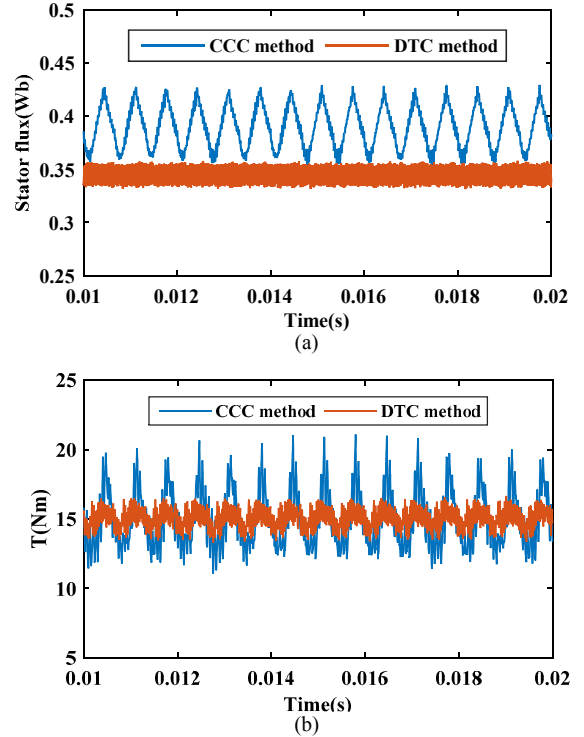

Fig. 7. Stator flux amplitude and total torque output of CCC and DTC method: (a) Stator flux amplitude, (b) Instantaneous torque

By plotting the flux onto an x-y stationary frame in Fig. 8, it is more obvious that the flux trajectory with the CCC method is a nonlinear hexagonal profile, whilst the DTC method produces a circular flux trajectory.
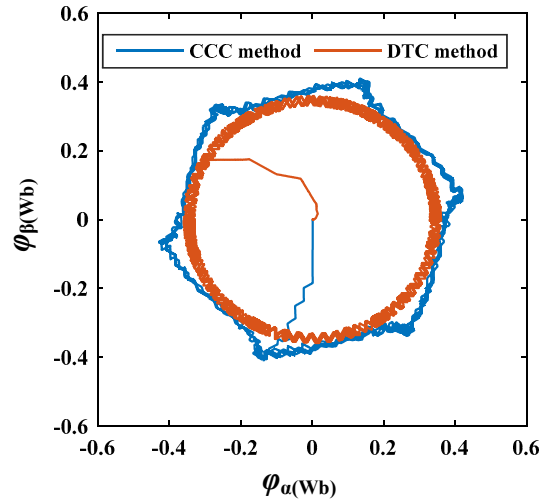

Fig. 8. Flux trajectory of CCC and DTC method

V. TEST RESULTS

In order to verify the proposed control method in a real-time system, a test rig is built with a six-phase 12/10 poles traditional SRM, a six-phase asymmetric half bridge IGBT inverter, a digital signal processor controller and a AC load machine. Test results are shown in Fig. 9. Six phase currents are shown in Fig. 9(a) and Fig. 9(b), which are comparable to the simulation results. Producing the same average torque of

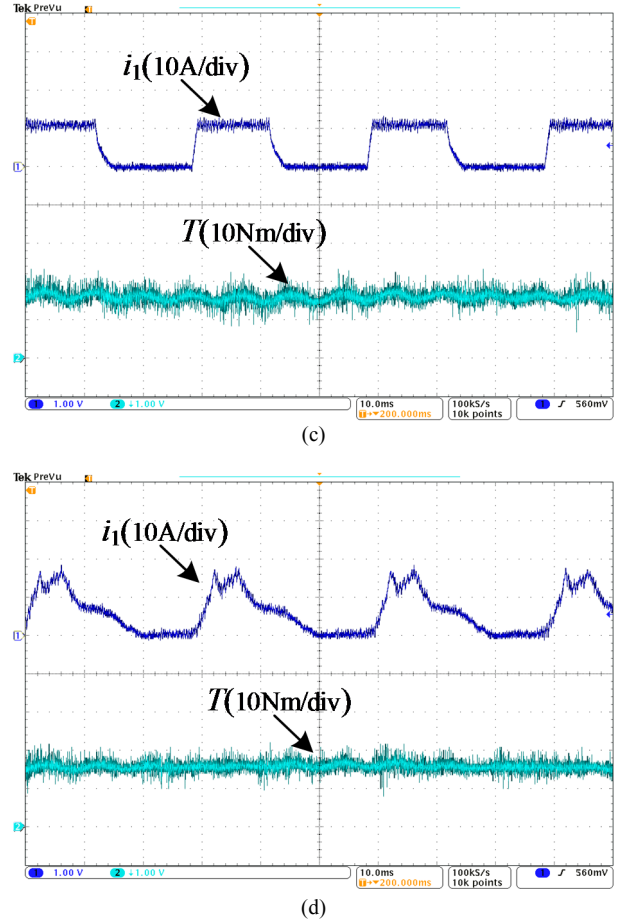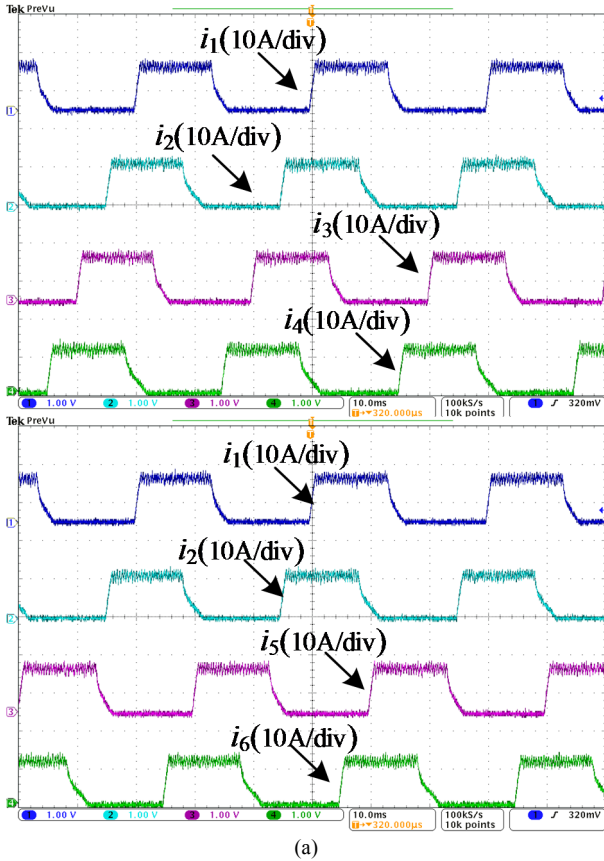15Nm in Fig. 9(c) and Fig. 9(d), DTC method reduces the torque ripple significantly compared with CCC method.

(a)

(b)

(c)

(d)

Fig. 8. Test results of CCC and DTC method: (a) phase current of CCC method, (b)phase current of DTC method, (c) torque output of CCC method, (d)torque output of DTC method

VI. Conclusions

In this paper a DTC method has been successfully applied to a six-phase 12/10 traditional SRM. With the DTC method the stator flux-linkage vector of the motor is kept constant by selecting an appropriate voltage vector, and instantaneous torque is controlled by accelerating or decelerating the stator flux vector relative to the rotor movement.

Compared with the traditional CCC method, producing the same average torque, the proposed DTC method can reduce torque ripple significantly.

VII. References

[1]   T. J. E. Miller, *Switched reluctance motors and their control*: Oxford Science Publications, 1999.

[2]   B. Bilgin, A. Emadi, and M. Krishnamurthy, "Comprehensive Evaluation of the Dynamic Performance of a 6/10 SRM for Traction Application in PHEVs," *Industrial Electronics, IEEE Transactions on,* vol. 60, pp. 2564-2575, 2013.

[3]   K. M. Rahman, B. Fahimi, G. Suresh, A. V. Rajarathnam, and M. Ehsani, "Advantages of switched reluctance motor applications to EV and HEV: design and control issues," *Industry Applications, IEEE Transactions on,* vol. 36, pp. 111-121, 2000.

[4]   J. F. Pan, N. C. Cheung, W. C. Gan, and S. W. Zhao, "A Novel Planar Switched Reluctance Motor for Industrial Applications," *Magnetics, IEEE Transactions on,* vol. 42, pp. 2836-2839, 2006.

[5]   K. Kiyota and A. Chiba, "Design of Switched Reluctance Motor Competitive to 60-kW IPMSM in Third-Generation Hybrid Electric

Vehicle," *IEEE Transactions on Industry Applications,* vol. 48, pp. 2303-2309, 2012.

[6] M. Takeno, A. Chiba, N. Hoshi, S. Ogasawara, M. Takemoto, and M. Rahman, "Test Results and Torque Improvement of the 50-kW Switched Reluctance Motor Designed for Hybrid Electric Vehicles," *IEEE Transactions on Industry Applications,* vol. 48, pp. 1327-1334, 2012.

[7] C. Hao and L. Shengli, "Fault Diagnosis Digital Method for Power Transistors in Power Converters of Switched Reluctance Motors," *Industrial Electronics, IEEE Transactions on,* vol. 60, pp. 749-763, 2013.

[8] S. Mir, M. S. Islam, T. Sebastian, and I. Husain, "Fault-tolerant switched reluctance motor drive using adaptive fuzzy logic controller," *Power Electronics, IEEE Transactions on,* vol. 19, pp. 289-295, 2004.

[9] I. Husain, "Minimization of torque ripple in SRM drives," *Industrial Electronics, IEEE Transactions on,* vol. 49, pp. 28-39, 2002.

[10] Y. K. Choi, H. S. Yoon, and C. S. Koh, "Pole-Shape Optimization of a Switched-Reluctance Motor for Torque Ripple Reduction," *IEEE Transactions on Magnetics,* vol. 43, pp. 1797-1800, 2007.

[11] L. Guangjin, J. Ojeda, S. Hlioui, E. Hoang, M. Lecrivain, and M. Gabsi, "Modification in Rotor Pole Geometry of Mutually Coupled Switched Reluctance Machine for Torque Ripple Mitigating," *Magnetics, IEEE Transactions on,* vol. 48, pp. 2025-2034, 2012.

[12] D. H. Lee, T. H. Pham, and J. W. Ahn, "Design and Operation Characteristics of Four-Two Pole High-Speed SRM for Torque Ripple Reduction," *IEEE Transactions on Industrial Electronics,* vol. 60, pp. 3637-3643, 2013.

[13] Y. Jin, B. Bilgin, and A. Emadi, "An Offline Torque Sharing Function for Torque Ripple Reduction in Switched Reluctance Motor Drives," *Energy Conversion, IEEE Transactions on,* vol. 30, pp. 726-735, 2015.

[14] B. Chunyuan, M. Yongkui, S. Chonghui, and R. Shuangyan, "Variable Structure Control of Switched Reluctance Motor and its Application," in *Intelligent Control and Automation, 2006. WCICA 2006. The Sixth World Congress on,* 2006, pp. 2490-2493.

[15] E. Daryabeigi, M. M. Namazi, A. Emanian, A. Rashidi, and S. M. Saghaian-Nejad, "Torque ripple reduction of switched reluctance motor (SRM) drives, with emotional controller (BELBIC)," in *Applied Power Electronics Conference and Exposition (APEC), 2012 Twenty-Seventh Annual IEEE,* 2012, pp. 1528-1535.

[16] R. S. Kumar and J. A. Vasanth, "Intelligent neuro controller based speed and torque control of five phase switched reluctance motor," in *Information Communication and Embedded Systems (ICICES), 2013 International Conference on,* 2013, pp. 966-973.

[17] J. A. Haylock, B. C. Mecrow, A. G. Jack, and D. J. Atkinson, "Operation of a fault tolerant PM drive for an aerospace fuel pump application," *Electric Power Applications, IEE Proceedings -,* vol. 145, pp. 441-448, 1998.

[18] T. Celik, "Segmental Rotor Switched Reluctance Drives," *Ph.D. Thesis,* Aug. 2011.

[19] J. D. Widmer, B. C. Mecrow, C. M. Spargo, R. Martin, and T. Celik, "Use of a 3 phase full bridge converter to drive a 6 phase switched reluctance machine," in *Power Electronics, Machines and Drives (PEMD 2012), 6th IET International Conference on,* 2012, pp. 1-6.

[20] J. D. Widmer, R. Martin, C. M. Spargo, B. C. Mecrow, and T. Celik, "Winding configurations for a six phase switched reluctance machine," in *Electrical Machines (ICEM), 2012 XXth International Conference on,* 2012, pp. 532-538.

[21] I. Takahashi and T. Noguchi, "A New Quick-Response and High-Efficiency Control Strategy of an Induction Motor," *Industry Applications, IEEE Transactions on,* vol. IA-22, pp. 820-827, 1986.

[22] L. Zhong, M. F. Rahman, W. Y. Hu, and K. W. Lim, "Analysis of direct torque control in permanent magnet synchronous motor drives," *Power Electronics, IEEE Transactions on,* vol. 12, pp. 528-536, 1997.

[23] A. D. Cheok and Y. Fukuda, "A new torque and flux control method for switched reluctance motor drives," *Power Electronics, IEEE Transactions on,* vol. 17, pp. 543-557, 2002.

VIII. BIOGRAPHIES

Xu Deng received the B.Eng. and M.Eng. degrees in Electrical Engineering from Nanjing University of Aeronautics and Astronautics, Nanjing, China, in 2010 and 2013, respectively.

She is currently working toward the Ph.D. degree as part of Electrical Power Research Group in the School of Electrical and Electronic Engineering, Newcastle University, Newcastle upon Tyne, U.K. Her main research is advanced control methods for power electronics and electric machines.

Barrie Mecrow received the Ph.D. degree from Newcastle University, Newcastle upon Tyne, U.K. He commenced his career as a Turbogenerator Design Engineer with NEI Parsons, Newcastle upon Tyne.

He became a Lecturer in 1987 and a Professor in 1998 with Newcastle University, where he is currently the Head of the School of Electrical and Electronic Engineering and a Professor of electrical power engineering. He is actively involved with industry in the aerospace, automotive, and consumer product sectors, which fund a wide range of projects. His research interests include fault-tolerant drives, high-performance permanent-magnet machines, and novel switched reluctance drives.

Shady Gadoue received the B.Sc. and M.Sc. degrees from Alexandria University, Alexandria, Egypt, in 2000 and 2003, respectively, and the Ph.D. degree from Newcastle University, Newcastle upon Tyne, U.K., in 2009, all in electrical engineering.

From 2009 to 2011, he was an Assistant Professor with the Department of Electrical Engineering, Alexandria University, where he was an Assistant Lecturer from 2000 to 2005. In 2011, he joined the Electrical Power Research Group, Newcastle University, as a Lecturer in Control Systems and Electric Drives. His main research interests include control, state and parameter identification, and optimization algorithms applied to energy conversion and motor drives systems.

Richard Martin received the M.Eng. degree in general engineering and the Ph.D. degree in electrical engineering from the University of Durham, Durham, U.K, in 2002 and 2007, respectively. His Ph.D. thesis was on the electromagnetic analysis and design of axial flux permanent-magnet machines.

He is a Senior Research Associate with Newcastle University, Newcastle-upon-Tyne, U.K., and his interests include permanent-magnet and switched reluctance machines.